# Photocatalytic decomposition and oxidation of dimethyl ether over Au/TiO$_2$

Gábor Schubert, Andrea Gazsi, Frigyes Solymosi *

*MTA-SZTE Reaction Kinetics and Surface Chemistry Research Group, University of Szeged, Rerrich Béla tér 1, H-6720 Szeged, Hungary*

ABSTRACT

The photocatalytic vapor-phase decomposition and oxidation of dimethyl ether were investigated on pure and Au-promoted TiO$_2$. Infrared spectroscopic studies revealed that dimethyl ether adsorbed on TiO$_2$-based catalysts undergoes partial dissociation to methoxy. Illumination induced a surface reaction and led to the formation of formate species. Whereas pure TiO$_2$ exhibited only a slight photoactivity, the deposition of Au on TiO$_2$ significantly enhanced the extent of the photocatalytic decomposition to yield H$_2$ and CO$_2$ with a small amount of CO. Addition of H$_2$O increased the extent of photocatalytic decomposition and eliminated the CO formed. A very high catalytic effect of Au/TiO$_2$ was observed in the photocatalytic oxidation of dimethyl ether to produce H$_2$ free of CO. When the bandgap of the TiO$_2$ support was lowered by N-doping from 3.02 eV to 1.98 eV, the photocatalytic decomposition and oxidation of dimethyl ether were observed even in visible light.

© 2014 Elsevier Inc. All rights reserved.

## 1. Introduction

Heterogeneous catalysis plays an important role in the synthesis of useful compounds and also in the destruction of pollutants. Most catalytic reactions proceed at elevated temperatures, even on active catalysts. This holds true for the catalytic decomposition of organic compounds to produce H$_2$. The pioneering work of Haruta et al. [1] and Hashmi and Hutchings [2] showed that supported Au in nanosize exhibited unusually high activity in several reactions. Illumination of Au/TiO$_2$ catalyst may provide a possibility to lower the reaction temperature and thereby to save energy [3–6]. In view of its high H/C ratio, dimethyl ether (DME) is a suitable compound for the production of H$_2$ [7]. This is reflected by the large number of works devoted to the study of the catalytic decomposition of DME [8–18]. Surprisingly, its photocatalytic decomposition and oxidation have received no attention so far [3–6]. It was recently found in our laboratory that the illumination of TiO$_2$-supported Pt metals induces the decomposition of DME at room temperature [19]. Rh/TiO$_2$ proved to be the most active catalyst. The small amount of CO formed can be diminished or eliminated by the addition of H$_2$O. As a continuation of our studies of the photocatalytic decomposition of HCOOH, C$_2$H$_5$OH and CH$_3$OH on Au/TiO$_2$ samples [20,21], we now present an account of the photocatalytic decomposition and oxidation of DME on a Au/TiO$_2$ catalyst.

Particular attention is paid to the effects of H$_2$O and to the influence of N-incorporation into the TiO$_2$; through the lowering of the bandgap, this may allow the photocatalytic reaction in visible light. The catalytic decomposition of DME on Au nanoparticles deposited on various oxides has been studied previously [18]. Au/CeO$_2$ was then found to be the most active catalyst, but even in this case the decomposition occurred with measurable rates only above 573 K.

## 2. Experimental

### 2.1. Methods

The photocatalytic reactions of DME were studied in the same way, as described in our previous papers [20,21]. We used a 15 W germicide lamp (type GCL 307T5L/CELL, Lighttech Ltd., Hungary), which emits predominantly in the wavelength range of 250–440 nm, its maximum intensity is at 254 nm. For the visible photocatalytic experiments, another type of lamp was used (Lighttech GCL 307T5L/GOLD) with 400–640 nm wavelength range and two maximum intensities at 453 and 545 nm. The approximate light intensity at the catalyst films is 3.9 mW/cm$^2$ for the germicide lamp and 2.1 mW/cm$^2$ for the other lamp.

For FTIR studies, a mobile IR cell housed in a metal chamber was used [20,21]. Samples were illuminated by the full arc of a Hg lamp (LPS-220, PTI) outside the IR sample compartment. Infrared spectra were recorded with a Biorad (Digilab. Div. FTS 155) instrument

with a wavenumber accuracy of ±4 cm$^{-1}$. All the spectra presented in this study are difference spectra. The determination of bandgaps of $TiO_2$ samples has been described in our previous work [22].

## 2.2. Materials

Supported Au catalysts were prepared by a deposition–precipitation method. $HAuCl_4$aq (p.a., 49% Au, Fluka AG) was first dissolved in triply distilled water. After the pH of the aqueous $HAuCl_4$ solution had been adjusted to 7.5 by the addition of 1 M NaOH solution, a suspension was prepared with the finely powdered oxidic support, and the system was kept at 343 K for 1 h under continuous stirring. The suspension was then aged for 24 h at room temperature, washed repeatedly with distilled water, dried at 353 K, and calcined in air at 573 K for 4 h. The following oxides were used as catalysts or supports: $TiO_2$ (Hombikat, UV 100, 200 m$^2$/g) and $SiO_2$ (Cabosil, 198 m$^2$/g). In addition, we also used a commercial 1% Au/$TiO_2$ (AUROlite, 50 m$^2$/g) sample. The sizes of the Au nanoparticles determined with an electron microscope: 1.5–2.0 nm for 1% Au/$TiO_2$ (Auro), 10–15 nm for 1% Au/$TiO_2$ (Hombi) and 6.0–7.0 nm for 1% Au/$SiO_2$ (Cabosil). For the preparation of N-doped $TiO_2$, we tested several methods. In one case, $TiO_2$ was treated with urea [23] and in other case with $NH_3$ [24,25]. The method developed by Beranek and Kisch [23] may be more effective for N-incorporation and lowering of the bandgap of $TiO_2$. The disadvantage of this methods is that the surface of $TiO_2$ is blocked by some CN containing residues formed in the decomposition of urea [24,26]. Therefore, we adopted the method of Xu et al. [25]. Accordingly, titanium tetrachloride was used as a precursor. After several steps, the $NH_3$-treated $TiO_2$ slurry was vacuum-dried at 353 K for 12 h, followed by calcination at 723 K in flowing air for 3 h. The bandgap of $TiO_2$ and $TiO_2$ + N was 3.02 eV and 1.98 eV, respectively [22]. The deposition of Au particles on these $TiO_2$ samples was carried out in the same way as described above. The sizes of Au were 18–20 nm. This sample is marked with "SX". The bandgap of Au/$TiO_2$ samples has been also determined. Deposition of Au on $TiO_2$ only slightly influenced the bandgap of $TiO_2$. We obtained values in the range of 3.04–3.07 eV. For photocatalytic measurements, the sample (70–80 mg) was sprayed onto the outer side of the inner tube from aqueous suspension. The catalysts were oxidized at 573 K and reduced at 573 K in the IR cell or in the catalytic reactor for 1 h.

## 3. Results

### 3.1. IR spectroscopic studies

The adsorption of DME on 1% Au/$TiO_2$ (Auro) produced strong absorption bands at 2950, 2879, 2838, 1469 and 1064 cm$^{-1}$ and weaker ones at 2910 and 1255 cm$^{-1}$. As a result of illumination, all these absorption bands underwent slow attenuation. A weak absorption band developed at 2937 cm$^{-1}$ and stronger ones at ∼1568, 1363 and 1045 cm$^{-1}$, which grew with the duration of illumination. In order to detect the CO formed, the sample was cooled to 200 K, when an absorption band at 2010 cm$^{-1}$ was identified. When Au/$TiO_2$ was illuminated in the presence of DME vapor, new absorption bands developed at 1570 and 1383 cm$^{-1}$, but the other spectral features remained practically unaltered. IR spectra are presented in Fig. 1A. Almost the same spectral features were observed on the $TiO_2$ (P25) used for the preparation of the 1% Au/$TiO_2$ (Auro) catalyst (Fig. 1B). The positions of the absorption bands observed and their possible assignments are presented in Table 1.

Because of the similarity of the IR spectra obtained on $TiO_2$ and Au/$TiO_2$, it is almost impossible to establish whether any adsorbed
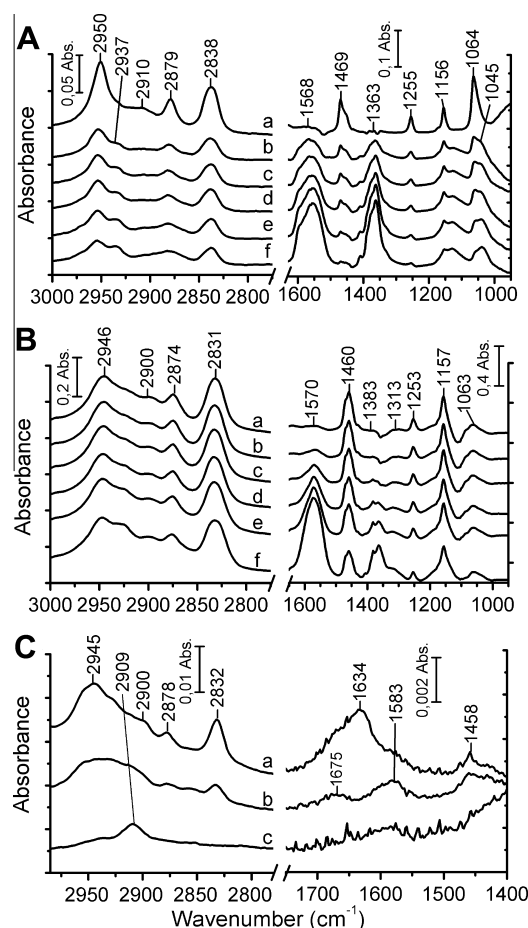


**Fig. 1.** Effects of illumination time on the IR spectra of adsorbed DME on $TiO_2$ (P25) (A); Au/$TiO_2$ (Auro) (B). Effects of heating of adsorbed DME on 5% Au/$SiO_2$ (C). 300 K (a); 373 K (b); 473 K (c). DME was adsorbed for 10 min at 300 K; afterward, the IR cell was degassed for 30 min before illumination. From time to time, the illumination was interrupted and the IR spectra were taken.

species are also bonded to Au particles. Application of $SiO_2$ as a support may provide a solution as DME, similarly to HCOOH, adsorbs weakly and non-dissociatively on the $SiO_2$ surface [18], as confirmed in the present study: degassing the adsorbed DME on $SiO_2$ at 423 K completely eliminated all the absorption bands. The adsorption of DME on 5% Au/$SiO_2$ gave absorption bands at 2945, 2871, 2912 and 2872 cm$^{-1}$. After heating of this sample to 373–473 K, a well-detectable band remained in the spectrum at 2909 cm$^{-1}$ and a very weak one at 1583 cm$^{-1}$ (Fig. 1C).

### 3.2. Photocatalytic decomposition of DME

The extent of the photocatalytic decomposition of DME on 1% Au/$TiO_2$ (Auro) attained 12% in 180 min (Fig. 2). The main products were $H_2$, $CO_2$ and CO, and trace amounts of $C_2H_4$, $CH_3OH$ and HCHO were also detected. The catalytic performance of the $TiO_2$ (P25) used for the preparation of the Au/$TiO_2$ (Auro) was also tested: the conversion of the DME then reached only ∼5% in the same reaction time. As in the other cases, a part of the $H_2$ formed reacted with $TiO_2$ [31,32]. The conversion remained below 10% on 1% Au/$TiO_2$ (Hombikat). For comparison, we determined the thermal decomposition of DME on the same Au/$TiO_2$ (Auro) film in the photocatalytic reactor. A measurable reaction, leading to 2.5% conversion, was measured at 573 K. A more significant decomposition (16% in ∼30 min) was attained at 623 K. The products were $H_2$, $CO_2$, $CH_4$, and $CH_3CHO$ in decreasing quantities (Fig. 3).

**Table 1**
Absorption bands observed following the adsorption of dimethyl ether and other compounds on different catalysts.[a]

| Vibrational mode | $DME_{(g)}$ [27] | DME on $TiO_2$ [present study] | DME on $Au/TiO_2$ [present study] | DME on $Rh/TiO_2$ [19] | DME on $Rh(1\,1\,1)$ [30] | $CH_3O_{(a)}$ on $TiO_2$ [28] | $CH_3O_{(a)}$ on $CeO_2$ [29] | $HCOO_{(a)}$ on $TiO_2$ [20] |
|---|---|---|---|---|---|---|---|---|
| $\upsilon_a(CH_3)$ | 2966 | 2950 | 2946 | 2952 | 2950 | 2965 | 2911 | 2958 |
|  | 2925 | 2921 | 2900 | 2906 |  | 2930 |  |  |
| $\upsilon_s(CH_3)$ | 2817 | 2878 | 2874 | 2879 |  | 2830 | 2803 | 2886 |
| $2\delta(CH_3)$ | 2887 | 2842 | 2831 | 2838 |  |  |  |  |
| $\upsilon_a(OCO)$ |  |  |  |  |  |  |  | 1552 |
| $\upsilon_s(OCO)$ |  |  |  |  |  |  |  | 1377 |
| $\delta_{as}(CH_3)$ | 1470 | 1459 | 1460 | 1458 | 1465 | 1462 | 1434 |  |
| $\delta_s(CH_3)$ | 1456 |  |  |  |  | 1436 |  |  |
| $\gamma(CH_3)$ | 1244 | 1253 | 1253 | 1253 | 1175 | 1151 |  |  |
|  | 1179 | 1159 | 1157 | 1153 |  |  |  |  |
| $\upsilon_{as}(CO)$ | 1102 | 1063 | 1063 | 1052 |  | 1125 | 1108 | 1277 |

[a] All IR spectra were registered at 300 K.

The addition of $H_2O$ to the DME markedly enhanced the extent of its photocatalytic decomposition (Fig. 4). At a 1:1 DME:$H_2O$ ratio, the conversion reached 55% and the formation of $H_2$ considerably increased. At the same time, no CO at all was present in the products. A very small amount of $C_2H_4$ was detected. An increase in the $H_2O$ content (DME:$H_2O$ ratio 1:5) did not result in any significant further change. Characteristic data are presented in Table 2.

We also examined the effects of $Al_2O_3$, earlier found to be an effective promoter for the thermal decomposition of DME [18]. When $Al_2O_3$ was mixed with 1% $Au/TiO_2$ in a 1:1 ratio, the extent of the photocatalytic decomposition of DME was enhanced by few percents. This appeared particularly obvious when the data were related to the amount of $Au/TiO_2$ present in the catalyst mixture.
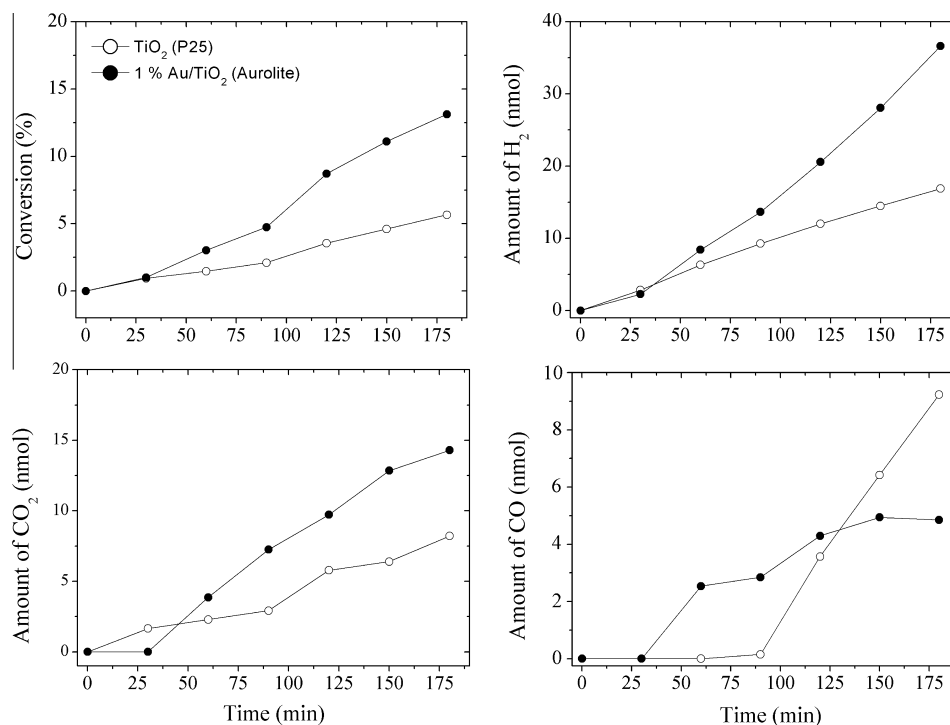
### 3.3. Photocatalytic oxidation of DME

Following the photolysis of coadsorbed of DME-$O_2$, only slight changes in the positions and intensities of the absorption bands were seen as a result of illumination. The same was true for the illumination of a 1:1 DME:$O_2$ gas mixture. However, intense bands developed at ∼1575 and ∼1365 cm$^{-1}$, which grew with the time of illumination. IR spectra are shown in Fig. 5.

The addition of $O_2$ markedly promoted the photo-induced reaction of DME. As shown in Fig. 6, the effect of $O_2$ appeared even at a DME:$O_2$ ratio of 1:0.2. Oxygen increased the conversion of DME and the amount of $H_2$ generated. The largest amount of $H_2$ was found at a DME:$O_2$ ratio of 1:1, when CO was completely absent from the products and the conversion of DME reached 60%. At a DME:$O_2$ ratio of 1:2, the conversion approached 100%, but the extent of the oxidation of $H_2$ also increased. Data relating to the selectivity and the yield of $H_2$ formation are also presented in Table 2. An interesting feature of the photocatalytic oxidation of DME is the production of $HCOOCH_3$ (Fig. 6D). It was formed in highest concentration at a DME:$O_2$ ratio of 1:2, but its production declined to a low level at progressively higher $O_2$ contents. The photocatalytic oxidation of DME occurred to relatively a low extent on pure $TiO_2$.

For comparison, we also studied the thermal oxidation of DME on 1% $Au/TiO_2$ (Auro) as a function of temperature. The reaction started at 523 K, and the conversion of DME was only ∼2% in ∼30 min. A more expressed level of oxidation, 60% conversion, was attained at 623 K. The only product of the oxidation was $CO_2$. The results are also presented in Fig. 3.



**Fig. 2.** Photocatalytic decomposition of DME on $TiO_2$ (P25) and $Au/TiO_2$ (Auro) catalysts.
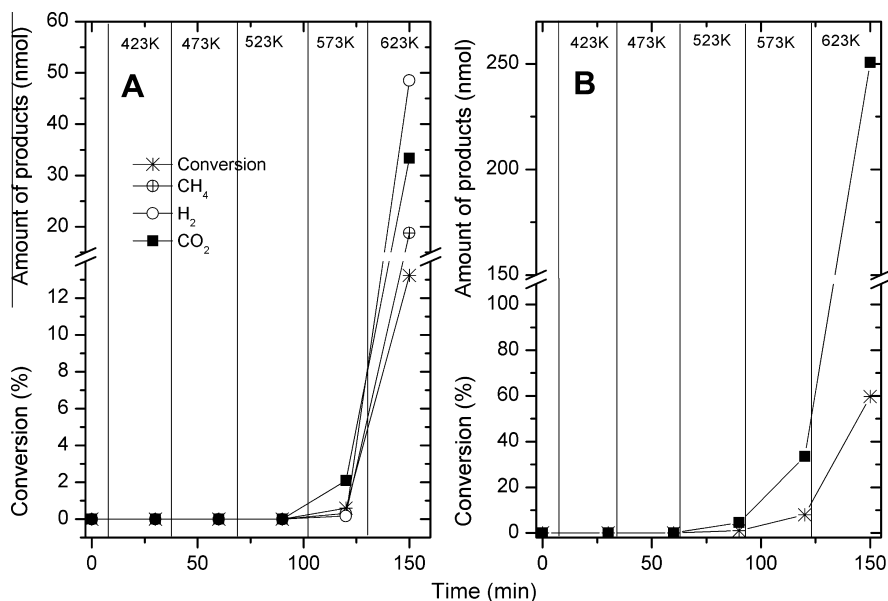
**Fig. 3.** Thermal decomposition (A) and oxidation (B) of DME on Au/TiO$_2$ (Auro) catalyst.

### 3.4. Studies in visible light

The photoreactions of DME were carried out with Au deposited on N-doped TiO$_2$. For comparison, we measured the photocatalytic decomposition of DME on Au deposited on undoped TiO$_2$ prepared in the same way. Au/TiO$_2$ samples prepared by the method of Xu et al. [25] exhibit always less photoactivity compared to that of the Au/TiO$_2$ (Auro) catalyst [20,21]. The advantageous effect of N-incorporation into the TiO$_2$ support already appeared in UV light: the conversion of DME was markedly higher on the N-doped catalyst. Experiments in visible light yielded similar results. Conversion data are presented in Fig. 7. It is important to note that the photoactivity of effective Au/TiO$_2$ (Auro) catalyst in visible light remained behind that of Au/TiO$_2$ + N (SX). The conversion of DME

in the decomposition was only 3.7–3.9%. In Table 3, we give the amounts of major products measured on N-doped and undoped Au/TiO$_2$ catalysts in the decomposition, reforming and oxidation of DME in visible light. It shows that the incorporation of N into TiO$_2$ appreciably enhanced the amount of H$_2$ formed.

## 4. Discussion

### 4.1. IR studies

The adsorption of DME on pure TiO$_2$ or 1% Au/TiO$_2$ gave very similar IR spectra. With regard to the characteristic spectral features of possible adsorbed species formed in the dissociation of
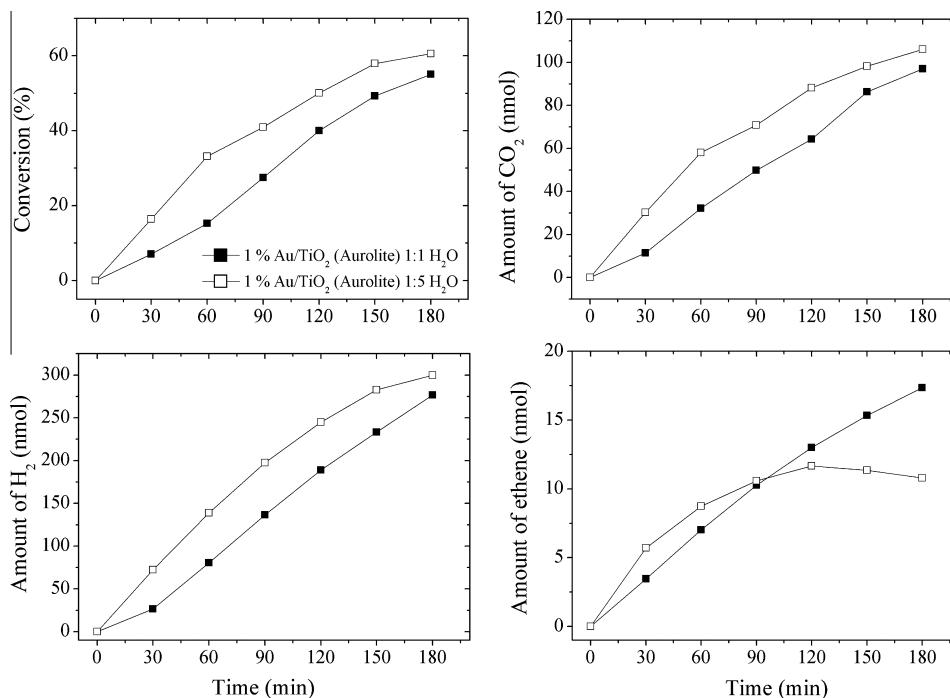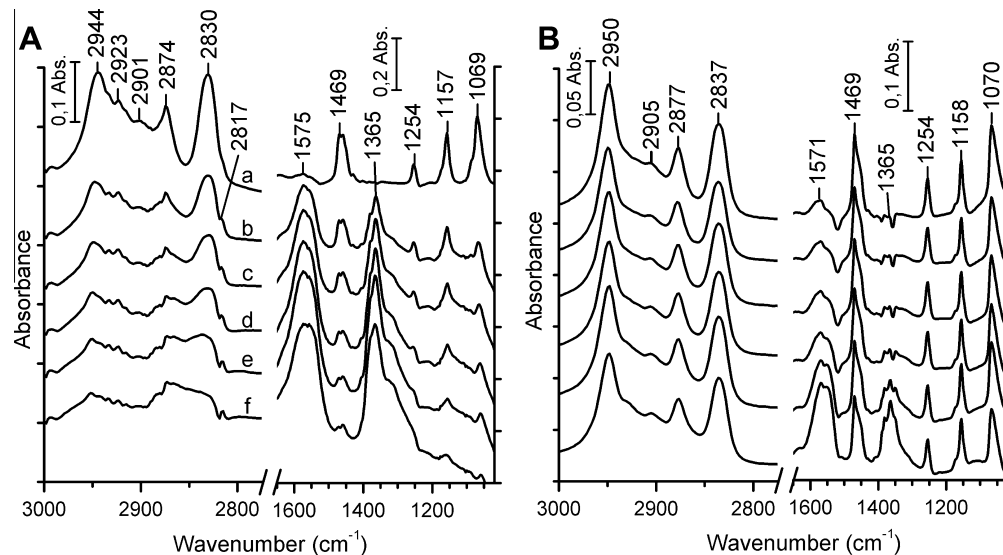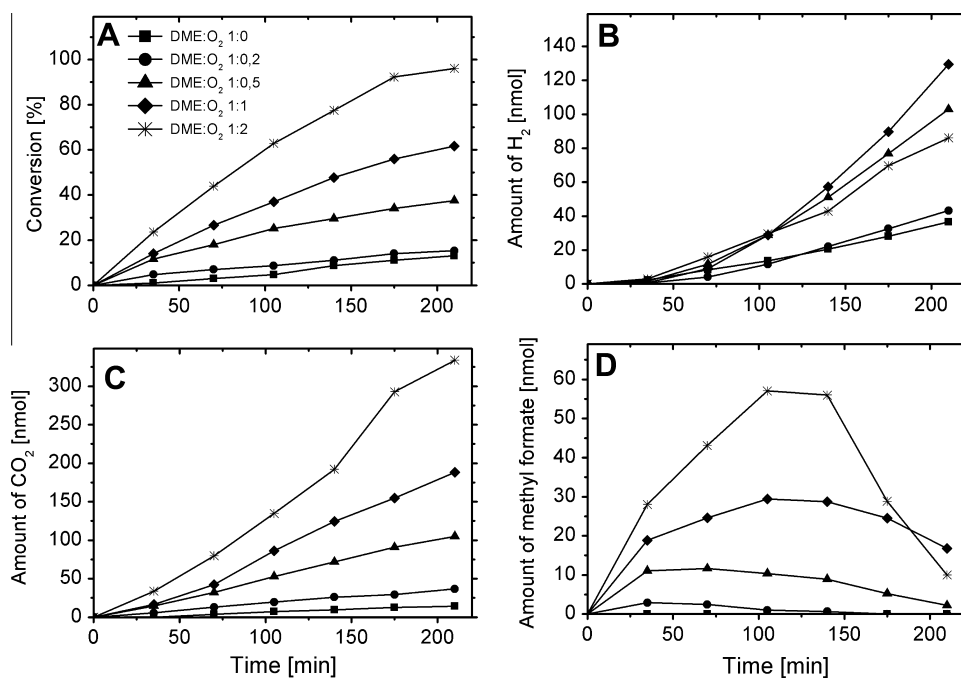


**Fig. 4.** Effects of H$_2$O on the photocatalytic decomposition of DME on Au/TiO$_2$ (Auro) catalyst.

**Table 2**
Some characteristic data for the photocatalytic decomposition and oxidation of DME on Au/TiO$_2$ (Auro) catalyst.[a]

|  | Decomposition DME:H$_2$O | | | Oxidation DME:O$_2$ | | |
|---|---|---|---|---|---|---|
|  | 1:0 | 1:1 | 1:5 | 1:0.5 | 1:1 | 1:2 |
| Conversion (%) | 11 | 55 | 60 | 32 | 56 | 92 |
| Selectivity for H$_2$ | 42 | 84 | 87 | 35 | 23 | 11 |
| Yield for H$_2$ | 4.7 | 46 | 53 | 12 | 13 | 10 |
| Maximum selectivity and yield for methyl formate | 2.5 | 0.23 | 1.45 | 30 | 35 | 40 |
|  | 0.3 | 0.11 | 0.48 | 5.3 | 13 | 25 |
| Amount of CO formed (%) | 9.6 | – | – | – | – | – |

[a] Data refer for 180 min of reaction time.



**Fig. 5.** Effects of illumination time on the IR spectra of DME:O$_2$ (1:1) co-adsorbed layer on Au/TiO$_2$ (Auro) (A) and in the presence of DME:O$_2$ (1:1) gas mixture (B). DME was adsorbed for 10 min at 300 K; afterward, the IR cell was degassed for 30 min before illumination. From time to time, the illumination was interrupted and the IR spectra were taken.



**Fig. 6.** Photocatalytic oxidation of DME on Au/TiO$_2$ (Auro) catalyst at different DME/O$_2$ ratios.
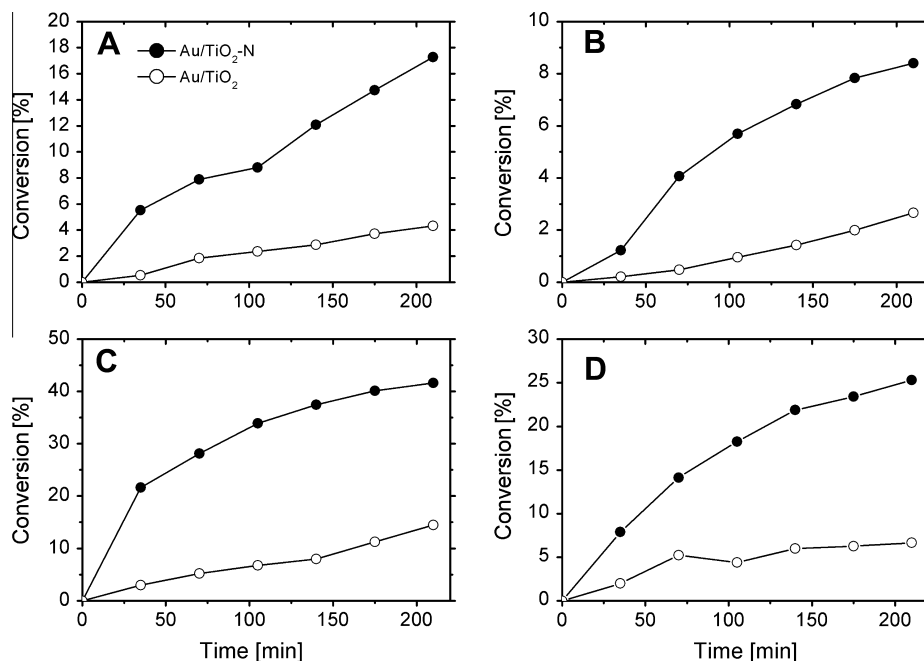
**Fig. 7.** Effects of N-doping of Au/TiO₂ (SX) on the photocatalytic decomposition (A and B) and photocatalytic oxidation (C and D) of DME in UV (A and C) and visible light (B and D).

**Table 3**
Some characteristic data for the photocatalytic reactions of DME on undoped and N-doped Au/TiO₂ (SX) in the visible light.[a]
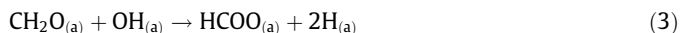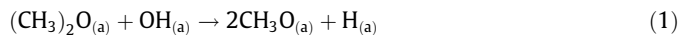
|  | Au/TiO₂ (SX) | | | Au/TiO₂ + N (SX) | | |
| --- | --- | --- | --- | --- | --- | --- |
|  | Decomposition | Reforming | Oxidation | Decomposition | Reforming | Oxidation |
| Conversion (%) | 2.5 | 8.0 | 6.0 | 8.4 | 16.0 | 25.0 |
| H₂ (nmol) | 1.2 | 26.0 | 0.5 | 33.0 | 68.0 | 20.0 |
| HCOOCH₃ (nmol) | 1.15 | 0.72 | 6.9 | 1.75 | 0.14 | – |
| CH₃CHO (nmol) | 0.63 | – | – | 1.04 | – | – |
| CO (nmol) | – | 3.0 | – | 3.0 | 2.0 | – |
| CO₂ (nmol) | 5.0 | 13.0 | – | 20.0 | 30.0 | 90.0 |

DME:H₂O = 1:1.
DME:O₂ = 1:0.5.
  [a] Data refer for 210 min of reaction time.

DME (Table 1), it may be concluded that the pair of bands at ∼2950 and 2838 cm⁻¹ are probably due to the vibration of molecularly adsorbed DME. The dissociation of adsorbed DME to furnish CH₃O species is indicated by the bands at ∼2937 and ∼2879 cm⁻¹. Disregarding the slight spectral changes resulting from illumination, there is no spectroscopic indication that illumination induces the dissociation of DME. However, the growing absorption bands due to HCOO species at ∼1568 and ∼1393 cm⁻¹ unambiguously point to the occurrence of a surface process induced by illumination. HCOO formation is described by the following steps:

$$(CH_3)_2O_{(a)} + OH_{(a)} \rightarrow 2CH_3O_{(a)} + H_{(a)} \tag{1}$$

$$CH_3O_{(a)} \rightarrow CH_2O_{(a)} + H_{(a)} \tag{2}$$

$$CH_2O_{(a)} + OH_{(a)} \rightarrow HCOO_{(a)} + 2H_{(a)} \tag{3}$$

$$CH_2O_{(a)} \rightarrow CO_{(a)} + 2H_{(a)} \tag{4}$$

When the system was allowed to cool, CO was adsorbed on Au particles, as indicated by a band at 2010 cm⁻¹.

The question of whether a fraction of the adsorbed DME or the CH₃O species was located on the Au particles remained open. As

the concentration of these adsorbed complexes is extremely small relative to the concentration of such complexes residing on TiO₂, we carried out IR spectroscopic studies on 5% Au/SiO₂, assuming that SiO₂ is an inert oxide from the aspect of the adsorbance of these species. The IR spectra in Fig. 1C allow the conclusion that small fractions of the CH₃O and HCOO species are bonded to Au particles. Accordingly, a part of the photochemical process may take place on Au particles.

### 4.2. Photocatalytic decomposition

Independently of its origin, pure TiO₂ exerted only very moderate activity on the photocatalytic decomposition of DME. The possible explanation is that the recombination of the charges induced by illumination:

$$TiO_2 + h\nu = h^+ + e^- \tag{5}$$

is very fast on TiO₂. Moreover, the dissociation of DME to the more reactive CH₃O species is very limited on TiO₂ as illustrated by the IR spectroscopic measurements. The deposition of Au on the TiO₂ significantly increased the extent of the photo-effect of TiO₂. The promoting effect of metals in photocatalytic reactions is generally explained by the better separation of the charge carriers formed

due to illumination [3–6], which provides a greater possibility for the formation of $CH_3O^-$:

$$CH_3O_{(a)} + e^- = CH_3O_{(a)}^{\delta-} \tag{6}$$

As the work function of Au (5.3 eV) is higher than that of $TiO_2$ (4.6 eV), the occurrence of electron transfer from $TiO_2$ to Au particles may be expected, leading to the extended activation of adsorbed molecules residing on the Au particles, or at the $Au/TiO_2$ interface. It may be recalled that this kind of electronic interaction between $TiO_2$ and metals was proposed first for the influence of a $TiO_2$ support on the catalytic performance of Ni and proved by changing the work function of $TiO_2$ by doping [33,34]. To our best knowledge, this was the first time when $TiO_2$ was used as a support. The role of the electronic interaction between metals and titana is now widely used in the explanation of the high photoactivity of metal-promoted $TiO_2$ [4–6,35,36]. It can be also assumed that the Schottky barrier at metal and $TiO_2$ interface can function as efficient barrier preventing electron–hole recombination [37,38]. In the case of gold catalyst Li et al. [39] pointed out that smaller metal particles induce more negative Fermi level shift than the larger particles. In addition, the surface plasmon resonance absorption may also contribute to the total absorption thereby to the enhanced photoactivity of $Au/TiO_2$ catalyst [5,6,40,41]. The higher photoactivity of $Au/TiO_2$ (Auro) compared to $Au/TiO_2$ (Hombi and SX) can be attributed to the smaller Au particles, which exhibited higher catalytic efficiency in several reactions [1,2].

The addition of $H_2O$ exerted a dramatic influence on the photocatalytic decomposition of DME, as indicated by the much higher conversion and by the increased amount of $H_2$ formation (Fig. 4). The selectivity of $H_2$ production reached even 87%. This influence can be attributed to the hydrolysis of DME and to the formation of the more reactive $CH_3OH$. As reported previously, $Au/TiO_2$ (Auro) is a very active catalyst for the photo-induced decomposition of $CH_3OH$ [21]. The total conversion of $CH_3OH$ was attained in ∼100 min. The promoting effect of the addition of $Al_2O_3$ to an $Au/TiO_2$ catalyst can be explained in the same way: because of its acidic sites, $Al_2O_3$ facilitates the hydrolysis of DME to $CH_3OH$. At the same time, in consequence of the water–gas shift reaction:

$$H_2O + CO = H_2 + CO_2 \tag{7}$$

$H_2O$ can reduce the amount of CO and increase that of $H_2$ formed. It appears that the illumination markedly promotes the water–gas shift reaction, which plays a dominant role in the elimination of CO formed.

The photocatalytic decomposition was also investigated on Au deposited on N-doped $TiO_2$. As shown in Fig. 7, the lowering of the bandgap of $TiO_2$ considerably enhanced the photoactivity of the $Au/TiO_2$ catalyst and allowed the reaction to occur even in visible light. This can be attributed to the significant reduction in the bandgap of $TiO_2$. Note that the deposition of Au onto $TiO_2$ did not alter the bandgap of $TiO_2$. Similar results were found by Ismail et al. [42] and Yu et al. [43]. These results are not surprising as the electric properties of n-type $TiO_2$ can be altered by doping only when the foreign ions are incorporated at least in the surface layer of $TiO_2$.
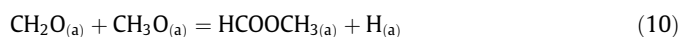
### 4.3. Photocatalytic oxidation

The addition of $O_2$ markedly enhanced the extent of DME that reacted in the photocatalytic process. Whereas in the absence of $O_2$ only ∼12% of the DME decomposed in 180 min, the decomposition approached 100% in the presence of a sufficient amount of $O_2$ (Fig. 6). Au nanoparticles have the noteworthy property of extremely high activity in oxidation processes. A good example is the catalytic oxidation of CO, which occurs even below room temperature [1,2,44–46]. Several explanations have been put forward for the high activity of the $Au/TiO_2$ catalyst, e.g. for the formation of $O_2^-$. The size of the Au particles, the active $Au/TiO_2$ interface and the electronic interaction between Au nanoparticles and n-type $TiO_2$ have been considered to play important roles in the activation of $O_2$. However, DME is a very unreactive molecule; its catalytic oxidation on $Au/TiO_2$ occurs only above 473 K (Fig. 5). Its oxidation at room temperature demands a high concentration of reactive $O_2^{\delta-}$, which is generated by illumination of the $DME/O_2$–$Au/TiO_2$ system. Accordingly, besides the reactions in Eqs. (2)–(7), the following step must be considered:
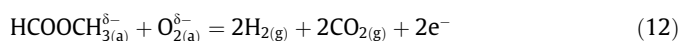
$$CH_3O_{(a)} + O_2^{\delta-} = H_{2(g)} + CO_{2(g)} + H_2O_{(g)} + e^- \tag{8}$$
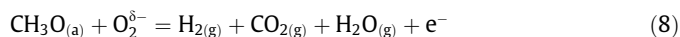
At higher $O_2$ content (a $DME:O_2$ ratio of 1:2), the oxidation of $H_2$ becomes more pronounced.

An interesting feature of the photocatalytic oxidation of DME is the transient formation of $HCOOCH_3$ (Fig. 6). As this compound was also detected in the photocatalytic decomposition of $CH_3OH$, it appears very likely that the same steps are responsible for its generation in the present case:

$$2CH_2O_{(a)} = HCOOCH_{3(a)} \tag{9}$$

$$CH_2O_{(a)} + CH_3O_{(a)} = HCOOCH_{3(a)} + H_{(a)} \tag{10}$$

As $Au/TiO_2$ is very active in the photocatalytic decomposition of $HCOOCH_3$ [47], it is not surprising that, after the DME has been consumed, the photo-induced reaction of $HCOOH_3$ takes place:

$$HCOOCH_{3(a)} + e^- = HCOOCH_{3(a)}^{\delta-} \tag{11}$$

$$HCOOCH_{3(a)}^{\delta-} + O_{2(a)}^{\delta-} = 2H_{2(g)} + 2CO_{2(g)} + 2e^- \tag{12}$$

An important result of the photocatalytic oxidation of DME is that CO is completely absent from the product, very likely as a result of its oxidation. In the optimum case, at an $DME:O_2$ ratio of 1.0:0.5 almost 35% of the H content of DME is converted into gaseous $H_2$ (Table 2). At a $DME:O_2$ ratio of 1:2, the oxidation of the H content of the DME becomes more pronounced.

As in the case of the photocatalytic decomposition of DME, lowering the bandgap of the $TiO_2$ greatly promoted the photocatalytic oxidation of DME on $Au/TiO_2$ in visible light.

## 5. Conclusions

1. IR spectroscopic studies revealed the partial dissociation of DME to methoxy species during adsorption on $TiO_2$ samples, which is only slightly influenced by illumination.
2. Au particles on $TiO_2$ significantly increased the extent of the photocatalytic decomposition of DME to produce mainly hydrogen. Adding $H_2O$ to DME markedly promoted the photocatalytic decomposition and eliminated the CO formed.
3. A very high conversion, 30–100%, was attained in the photocatalytic oxidation of DME on $Au/TiO_2$. CO completely disappeared from the products.
4. Lowering the bandgap of $TiO_2$ by N-doping allowed the occurrence of the photoreactions in the visible light.

# References

[1] M. Haruta, T. Kobayashi, H. Sano, N. Yamada, Chem. Lett. (1987) 405.
[2] A.S.K. Hashmi, G.J. Hutchings, Angew. Chem. Int. Ed. 45 (2006) 7896.
[3] A. Linsebigler, G. Lu, J.T. Yates Jr., Chem. Rev. 95 (1995) 735.
[4] M.R. Hoffmann, S.T. Martin, W. Choi, D.W. Bahnemann, Chem. Rev. 95 (1995) 69.
[5] V. Subramanian, E.E. Wolf, P.V. Kamat, J. Am. Chem. Soc. 126 (2004) 4943.
[6] A. Primo, A. Corma, H. Garcia, Phys. Chem. Chem. Phys. 13 (2011) 886.
[7] G.A. Olah, Á. Molnár, Hydrocarbon Chemistry, Wiley, New York, 2003. and references therein.
[8] V.V. Galvita, G.L. Semin, V.D. Belyaev, T.M. Yurieva, V.A. Sobyanin, Appl. Catal. A Gen. 216 (2001) 85.
[9] K. Takeishi, H. Suzuki, Appl. Catal. A Gen. 260 (2004) 111.
[10] T. Nishiguchi, K. Oka, T. Matsumoto, H. Kanai, K. Utani, S. Imamura, Appl. Catal. A Gen. 301 (2004) 66.
[11] K. Faungnawakij, Y. Tanaka, N. Shimoda, T. Fukunaga, S. Kawashima, R. Kikuchi, K. Eguchi, Appl. Catal. A Gen. 304 (2006) 40.
[12] T. Kawabata, H. Matsuoka, T. Shishido, D. Li, Y. Tian, T. Sano, K. Takehira, Appl. Catal. A Gen. 308 (2006) 82.
[13] T.A. Semelsberger, K.C. Ott, R.L. Borup, H.L. Greene, Appl. Catal. B Environ. 61 (2005) 281;
T.A. Semelsberger, K.C. Ott, R.L. Borup, H.L. Greene, Appl. Catal. B Environ. 65 (2005) 291.
[14] T. Fukunaga, N. Ryomon, S. Shimazo, Appl. Catal. A Gen. 348 (2008) 193.
[15] F. Solymosi, R. Barthos, A. Kecskeméti, Appl. Catal. A Gen. 350 (2008) 30.
[16] Gy. Halasi, T. Bánsági, F. Solymosi, ChemCatChem 1 (2009) 311.
[17] K. Faungnawakij, N. Shimoda, T. Fukunaga, R. Kikuchi, K. Eguchi, Appl. Catal. B Environ. 92 (2009) 341. and references therein.
[18] A. Gazsi, I. Ugrai, F. Solymosi, Appl. Catal. A Gen. 391 (2011) 360.
[19] Gy. Halasi, G. Schubert, F. Solymosi, The application of photocatalysis in chemistry, AJAC, in press (special issue).
[20] A. Gazsi, G. Schubert, P. Pusztai, T. Bánsági, F. Solymosi, Int. J. Hydrogen Energy 38 (2013) 3756.
[21] A. Gazsi, G. Schubert, T. Bánsági, F. Solymosi, J. Photochem. Photobiol. A Chem. 271 (2013) 45.
[22] Gy. Halasi, I. Ugrai, F. Solymosi, J. Catal. 281 (2011) 309.
[23] R. Beranek, H. Kisch, Photochem. Photobiol. Sci. 7 (2008) 40.
[24] O. Diwald, T.L. Thompson, T. Zubkov, G. Goralski, S.D. Walck, J.T. Yates, J. Phys. Chem. B 108 (2004) 6004.
[25] J.-H. Xu, W.-L. Dai, J. Li, Y. Cao, H. Li, H. He, K. Fan, Catal. Commun. 9 (2008) 146.
[26] Gy. Halasi, G. Schubert, F. Solymosi, J. Phys. Chem. C 116 (2012) 15396.
[27] J.G. Chen, P. Basu, T.H. Ballinger, J.T. Yates Jr., Langmuir 5 (1989) 352.
[28] G. Busca, A.S. Elmi, P. Forzatti, J. Phys. Chem. 91 (1987) 5263.
[29] A. Badri, C. Binet, J.C. Lavalley, G. Blanchard, J. Chem. Soc. Far. Trans. 93 (1997) 1159.
[30] L. Bugyi, F. Solymosi, Surf. Sci. 385 (1997) 365.
[31] K.L. Miller, C.W. Lee, J.L. Falconer, J.W. Medlin, J. Catal. 275 (2010) 294.
[32] S.S. Malwadkar, R.S. Gholap, S.V. Awate, P.V. Korake, J. Photochem. Photobiol. A Chem. 203 (2009) 24.
[33] Z.G. Szabó, F. Solymosi, Actes Congr. Int. Catalyse 2e Paris (1961) 1627.
[34] F. Solymosi, Catal. Rev. 1 (1968) 233.
[35] P. Wang, B. Huang, Y. Dai, M.-H. Whaghbo, Phys. Chem. Chem. Phys. 14 (2012) 9813.
[36] P.V. Kamat, J. Phys. Chem. Lett. 3 (2012) 663.
[37] A.A. Ismail, D.W. Bahnemann, I. Bannat, L. Wark, M. Gold, J. Phys. Chem. C 113 (2009) 7429.
[38] M. Alvaro, B. Cojocaru, A.A. Ismail, N. Petrea, B. Ferrer, F.A. Harraz, V.I. Parvulescu, H. Garcia, Appl. Catal. B Environ. 99 (2010) 191.
[39] G. Wu, T. Chen, W. Su, G. Zhou, X. Zong, Z. Lei, C. Li, Int. J. Hydrogen Energy 33 (2008) 1243.
[40] K. Ueno, H. Misawa, J. Photochem. Photobiol. C Photochem. Rev. 15 (2013) 31.
[41] K. Yu, Y. Tian, T. Tatsuma, Phys. Chem. Chem. Phys. 8 (2006) 5417.
[42] A.A. Ismail, D.W. Bahnemann, I. Bannat, M. Wark, J. Phys. Chem. C 113 (2009) 7429.
[43] J. Yu, L. Yue, S. Liu, B. Huang, X. Zhang, J. Colloid Interface Sci. 334 (2009) 58.
[44] M. Haruta, Catal. Today 36 (1997) 153.
[45] M. Valden, X. Lai, D.W. Goodman, Science 281 (1998) 1647.
[46] F. Boccuzzi, A. Chiorino, M. Manzoli, P. Lu, T. Akita, S. Ichikawa, M. Haruta, J. Catal. 202 (2001) 256.
[47] A. Gazsi, G. Schubert, P. Pusztai, F. Solymosi, Int. J. Hydrogen Energy 38 (2013) 7756.